H.C. Siegmann
M. Kasper, K. Sattler, K. Siegmann
ETH Zürich
Laboratory for Combustion Aerosols
and Suspended Particles
CH Zurich

Formation of Carbon in Combustion: The Influence of Fuel Additives

Formation of Carbon in Combustion: The Influence of Fuel Additives

M. Kasper[1], K. Sattler[2], K. Siegmann[1‡], and H.C. Siegmann[1]

[1] ETH-Zürich, Laboratory for Combustion Aerosols and Suspended Particles, 8093 Zürich, Switzerland
[2] University of Hawaii, Department of Physics and Astronomy, Watanabe Hall / 2505 Correa Road, Honolulu Hawaii 96822, USA

Proceedings of the Workshop on Particle Measurement at ETH Zürich, August 7, 1997

Abstract - We show that the fuel additive ferrocene leads to the formation of condensation nuclei in the combustion zone prior to the formation of carbonaceous particles. The condensation nuclei most likely are iron oxides. The carbonaceous matter preferentially condenses at the surface of the iron oxide nuclei where it is burnt in the last stage of the combustion. Under the ideal conditions of a laminar acetylene flame diluted with argon almost complete burnout of the carbonaceous matter is achieved. In turbo-charged heavy duty diesel construction engines, the same basic phenomena are observed, yet the burnout is far from complete.

Introduction

Fuel additives have always played an important role in combustion. For instance, lead compounds have been added to the gasoline to reduce the knocking in spark ignition engines. Yet this technology had to be abandoned because lead containing chemicals are immitted with the exhaust into the air in which we live, and such chemicals are toxic for humans. Recently, it has been recognized that carbonaceous particulate matter immitted by diesel engines constitutes a significant health hazard too. Fuel additives such as ferrocene $Fe(C_5H_5)_2$ are able to reduce these immissions. However, the transition metal (Fe) reappears in the form of very fine respiratory oxide nuclei in the exhaust and has to be captured in an efficient ceramic or fiber filter to prevent immission into the ambient air. It has been shown that with this concept, one can effectively reduce the particulate immissions for instance from heavy duty construction engines [1, 2].
In this paper, we try to understand the mechanism by which ferrocene reduces carbonaceous matter in combustion. Detailed knowledge of the underlying processes can help to apply the technology more effectively and to control its proper functioning. We will show that heterogeneous catalysis comes into play, that is the iron is present in the

‡. To whom correspondence should be addressed.

form of very fine nuclei in the combustion zone rather than as ion or vapor. We will further show that the reduction of the carbonaceous matter in the exhaust is caused by more efficient burnout rather than by inhibition of the formation of carbon.
The main innovation by which these new results are obtained is based on the photoemission of electrons from the particles in their natural gaseous environment. Our work differs from numerous other experiments in that we do not precipitate the particles onto a substrate prior to photoemission spectroscopy. With the technique of photoelectric charging of the particles, we obtain a fingerprint of the chemical state of the particle surface as it depends on the time spent in the combustion zone.

Observation of size resolved surface chemistry on ultrafine particles

The present work employs a somewhat different experimental technique compared to conventional combustion research in that we take tiny samples of gas containing molecules and particles directly from the combustion zone. The sampled volumes are immediately and highly diluted with inert gas such as N_2 and subsequently fed either into a time of flight (TOF) mass spectrometer or into aerosol sizing equipment (DMA). We develop the basic understanding first on a model combustion. For this, we have chosen a laminar diffusion flame burning with simple gaseous fuels such as methane (CH_4) or acetylene (C_2H_2). However, the technique may be applied to almost any combustion, be it wood or coal fire, diesel engine, cigarette, or whatever else one likes to imagine. Yet the model combustion has the advantage of establishing a time scale by the laminar flow. The distance from the orifice of the burner to the location of the sampling can be translated into a time spent in the combustion zone. As the oxygen is supplied by diffusion from the outside, the symmetry axis in the middle of the flame has the lowest oxygen partial pressure. The results discussed below are valid for the symmetry axis of the cylindrical flame. To avoid flickering of the flame, it is surrounded by a laminar flow of air.
In Fig. 1, we show the complete experimental setup (excluding the TOF which is described in [3]). It consists of two parts: the combustion and sampling, and the measurement of the size resolved surface chemistry of the particles. The sample extraction system consists of a tube placed across the flame in which the dilution gas N_2 flows at a slightly reduced pressure. Depending on the pressure difference between flame and dilution gas stream, flame gases enter the tube through a pinhole at the bottom. The position of the pinhole in the flame is adjusted by moving the flame with a computer driven mechanical motion. It is thus possible to take samples from any point in the flame. We can show that the height resolution of the sampling is better than 0.1 mm. The visible height of the flame is adjusted to 70 mm.
The gaseous fuel CH_4 or C_2H_2 is preheated and can be diluted with Ar which increases the temperature and slows down the formation of carbonaceous particles. A crucible containing ferrocene is placed in the preheated stream of the fuel. At temperatures ranging from 50 - 100 ^{o}C, ferrocene vapor is added to the fuel gas. Alternatively,

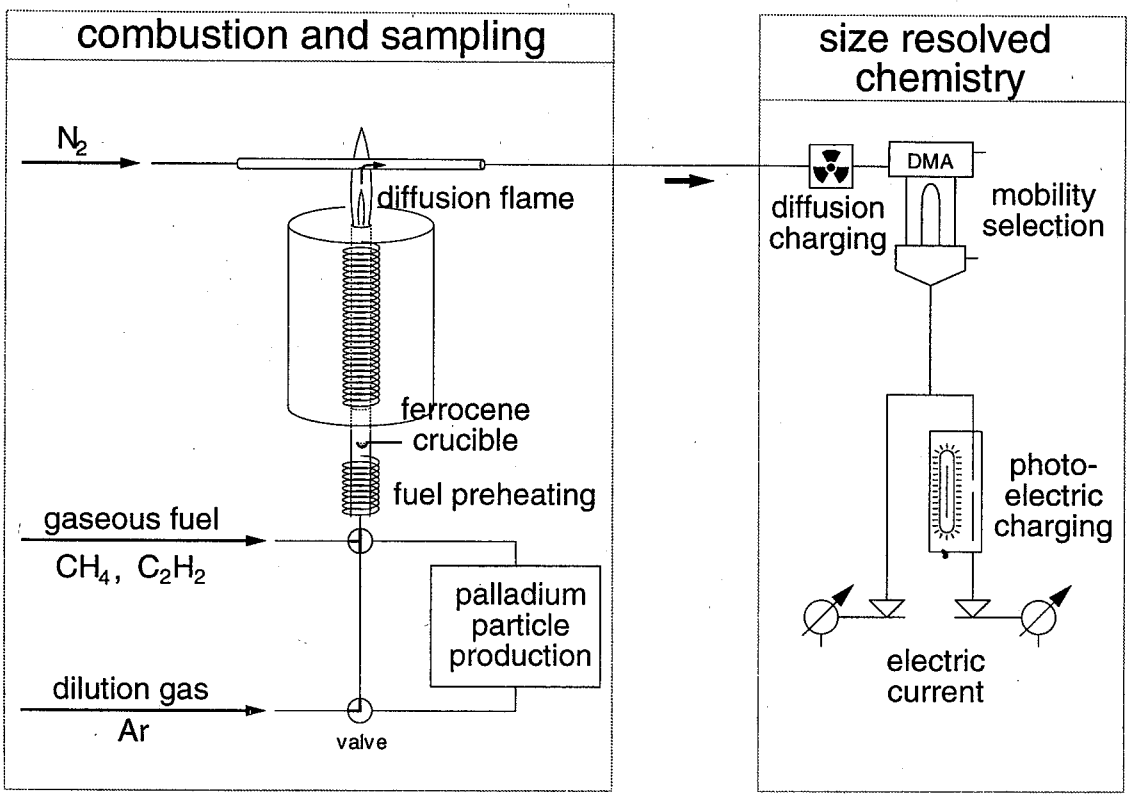

Figure 1: Experimental set-up. The model combustion is a stabilized laminar diffusion flame. Tiny volumes of gas containing the flame generated particles and molecules are extracted through a pinhole and immediately diluted. The size resolved analysis of the particles and their surface is described in the text.

palladium particles can be added. These particles are produced by heating a palladium wire in argon. A filter removes the particles if desired without changing the argon dilution.

Seeding the fuel with palladium particles of known size distribution is important to test the extraction system, particularly the question of whether the particle size distribution measured in the extracted and diluted gas is the same as that in the flame. One can perform three different tests: 1. extract samples from the non-ignited Ar/fuel mixture; 2. extract samples from the flame without palladium particles; 3. extract samples from the flame with the palladium particles added to the fuel gas. The summary of these tests is that the size distribution of the palladium particles remains the same with the exception of shrinkage of the large palladium particles in the flame. The shrinkage occurs naturally when the large palladium agglomerates are exposed to high temperatures [4].

The dilution gas N_2 containing the particles from the combustion zone is then entering the equipment for observation of size resolved surface chemistry. The aim is now to investigate the surface properties and condensation of chemicals onto the particles nucleated in the flame. The gas stream carrying the particles first enters a diffusion charger and subsequently a differential mobility analyzer (DMA).

This standard equipment selects particles with one negative electrical charge and one specific electrical mobility diameter D which is chosen according to the voltage V applied to the DMA. After that, the gas stream carries monodisperse singly charged particles. It is then split into two equal streams, one of which passes directly through a filter catching all particles. The electric current flowing from the filter to ground potential as measured with a femto-amperemeter yields the concentration of the particles at the mobility diameter D. Plotting the voltage V on the DMA vs. the filter current yields the size distribution of the particles. The other half of the gas stream passes by a source of ultraviolet light.

The energy of this light is lower than the energy required to ionize the molecules of the gas carrying the particles, but higher than the photoelectric work function of the particles. Under these conditions, photoelectrons may be emitted from the particles depending on their photoelectric yield. The photoelectrons from the particles are removed by an alternating electric field which leaves the particles that emitted the photoelectrons within the gas stream. After this photoelectric charging, the gas carrying the particles enters a second filter with femto-amperemeter. The differential current of the branch with and the one without photoelectric emission is proportional to the photoelectric yield. This gives a fingerprint of the chemical composition of the surface layers of the particles as it depends on the particle size.

In Fig. 2 are shown the results obtained with a high pressure Hg-arc and with palladium particles of diameter $D = 39$ nm in the Methane flame. These particles were added to the fuel gas as described above. In the non-ignited gas flow, the photoelectric yield does not change with the height above the burner orifice as expected. However, in the flame the palladium particles reduce their yield from $HaB = 10$ mm onwards. At about $HaB = 30$ mm, the yield reaches its minimum, but increases on increasing HaB. At $35 \leq HaB \leq 70$, the palladium particles are buried in the flame generated particles [4] and therefore cannot be identified any more. When the palladium particles reappear at $HaB = 70$ mm, they are in the low yield phase.

Photoelectron yield spectroscopy can be interpreted on a phenomenological basis only. In any case, it is a very fine sensor of the surface properties, responding to adsorbates at coverages at and below the monolayer level. The surface of palladium has been studied in detail since it is one of the key catalysts of heterogeneous reactions. Based on the extensive experience with this model surface, we propose the following explanation for the observations of Fig. 2. The initial decrease of the yield indicates the availability of carbon in the combustion. The formation of graphitic carbon at the surface of palladium is known to induce a substantial reduction of the photoelectric yield as observed. The subsequent increase of the yield at $HaB \geq 35$ mm occurs at the onset of the formation of polycyclic aromatic hydrocarbons (PAH) in the methane flame [5]. These PAH adsorb on the surface of the palladium particles on their way to the photoemission tube. When the

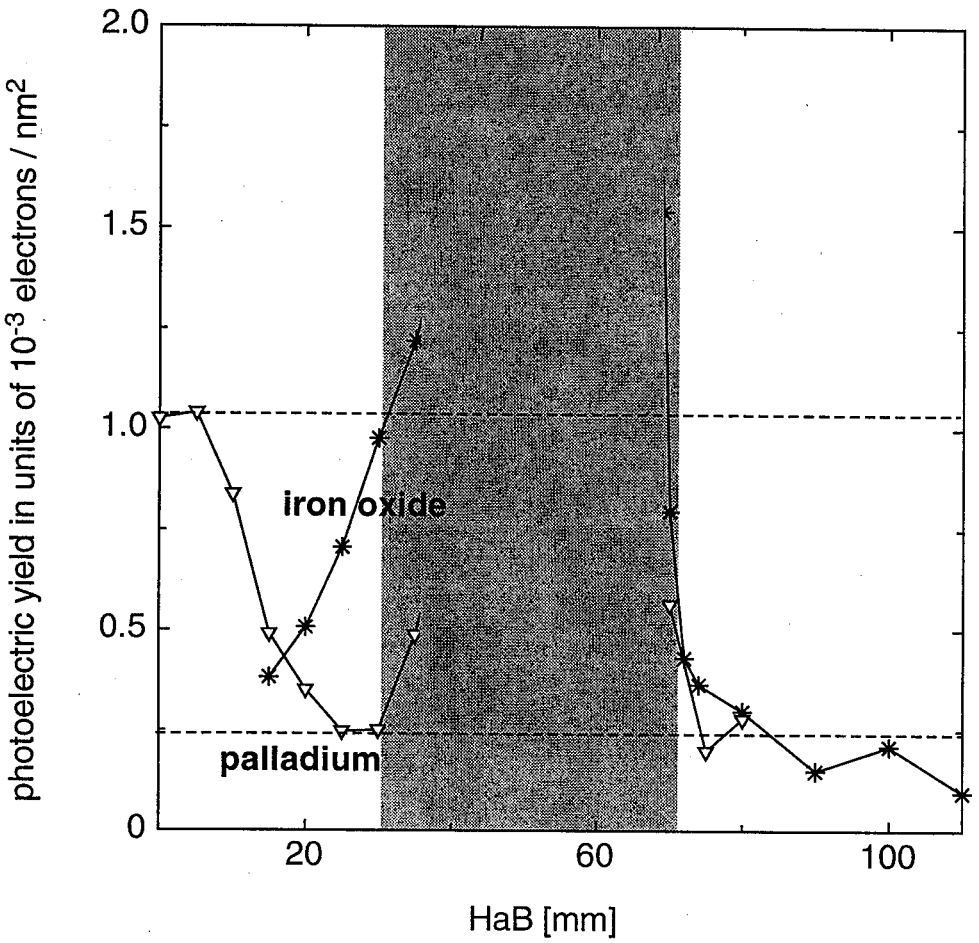

Figure 2: The photoelectric yield of electrons per unit particle surface as produced by palladium and iron oxide nuclei with a Hg high pressure arc is plotted vs. the height HaB above the orifice of the burner. On the gray region, carbonaceous particles are so numerous that the palladium particles and the iron oxide nuclei cannot be separately observed. The measurements are done with a methane flame diluted with argon.

PAH have disappeared at the top of the flame, the yield of the palladium particles is still low because the coverage of the palladium surface with graphitic carbon persists. This is consistent with the well known fact that graphitic carbon, once deposited at the surface of a metal, is very hard to remove. In conclusion we see that the palladium surface conveys a picture of the chemistry in the flame, in particular it clearly marks the soot inception point at *HaB* = 30 mm where carbon becomes available in large quantities.
We proceed now to the yield of particles in the CH_4-flame without palladium particles, but with ferrocene vapor added to the fuel gas. In the flame with ferrocene vapor, the first particles appear already at *HaB* = 20 mm. These particles are not carbonaceous soot particles, because their photoelectric yield is 10 times lower. Most likely, these are iron

oxide particles formed from the Fe-ions liberated when the ferrocene molecules are cracked. Without cracking, that is in the non-ignited gas flow, no particles appear. Furthermore, the iron oxides are known to exhibit high work function and low photoelectric yield. These iron oxide particles increase their yield as *HaB* increases approaching the yield of the carbonaceous soot particles after the soot inception point. This shows that the iron oxide particles act as condensation nuclei for the carbonaceous particles as their surface cannot be distinguished any more from the one of the genuine soot particles. After the soot burnout at $HaB \geq 70$ mm, the iron oxide particles reappear with their original low yield that continues a slow decrease as the flame gases age. The fast drop of the yield at the burnout of the soot particles suggests that the carbonaceous matter that condensed on the iron oxide nuclei surface was burnt. The slow decrease of the yield at $HaB \geq 80$ mm could indicate complete oxidation or a change of the oxidation state of the iron oxide particles. The results shown in Fig. 2 were obtained with iron oxide nuclei of $D = 20$ nm. Note the difference between the behavior of palladium particles compared to the one of the Iron oxide particles: While the palladium particles require a permanent coverage of the surface when passing through the flame, the iron oxide particles return to their original state after the burnout, that is all the carbon deposited at their surface is burnt at the end of the flame.

Size distributions of iron oxide nuclei and carbonaceous particles

As the photoelectric yield Y_{C+PAH} of the carbonaceous particles is 10 times higher compared to the yield Y_{FeO} of the iron oxide nuclei, one can calculate what fraction a of the available surface provided by all particles is still uncovered iron oxide.
The size dependent total yield Y_{tot} of all particles is obtained directly in the experiment. We have the following equation:

$$Y_{tot} = \alpha Y_{FeO} + (1 - \alpha) Y_{C+PAH} \qquad (1)$$

To apply eqn (1), we assume that $Y_{FeO} = const$, while the height dependence of Y_{C+PAH} is determined by the measurement of the particles from a flame not seeded with ferrocene vapor.
Fig. 3 shows results obtained with an Ar-diluted methane flame that was seeded with ferrocene vapor. Eqn (1) has been used to calculate from the observed Y_{tot} and the total number of particles at each particle diameter D the fraction a of particles with iron oxide type surfaces and the fraction a of particles with carbonaceous type surface. For comparison, the size distributions of particles extracted from the unseeded flame are also shown.
At $HaB = 20$ mm, only iron oxide type nuclei are present while carbonaceous particles are still absent. The small average diameter of the iron oxide nuclei and the shape of the spectrum suggests that these nuclei are growing by surface condensation of atoms and/or molecules. The iron oxide particles continue to increase in size as well as in number ($HaB = 35$ mm). At 50 mm *HaB* they begin to disappear because they get covered with

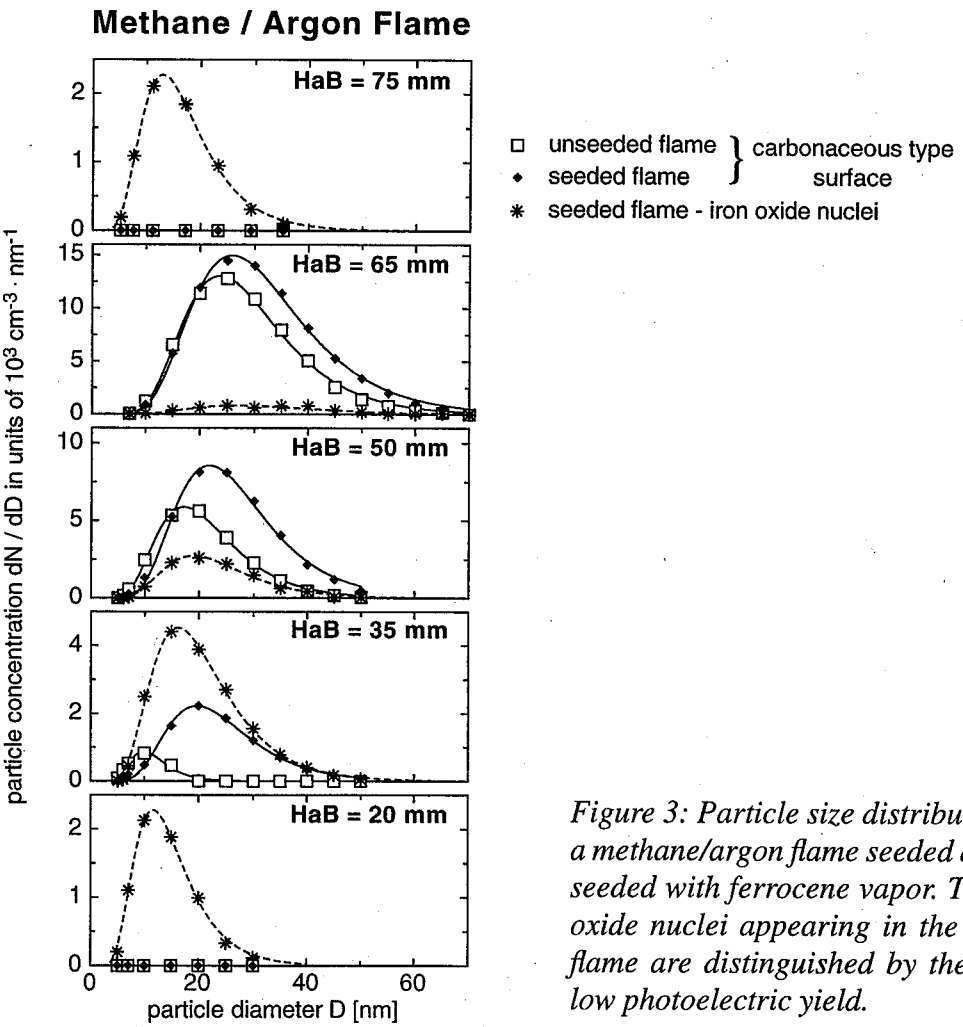

Figure 3: Particle size distributions in a methane/argon flame seeded and unseeded with ferrocene vapor. The iron oxide nuclei appearing in the seeded flame are distinguished by their very low photoelectric yield.

carbonaceous material, until in the soot rich region of the flame around *HaB* = 65 mm basically no particles with an iron oxide surface are left. At *HaB* = 75 mm, the carbonaceous matter disappears by burnout and the iron oxide nuclei reappear almost with their original size distribution, and with their original state of the surface.
The seeded flame seems to have more and larger carbonaceous particles compared to the unseeded flame. This suggests that the condensation of carbonaceous material occurs preferentially at the surface of the iron oxide nuclei. While the difference between seeded and unseeded flame is greatest at lower heights, that is near the soot inception point, the difference introduced by seeding is small at *HaB* = 65 mm, the height of the largest concentration of carbonaceous matter. This clearly shows that ferrocene has hardly any influence on the total amount of carbonaceous matter produced in the flame.
Since the methane flame does not emit any carbonaceous particles, we demonstrate the burnout induced by the ferrocene with a soot emitting flame. To this end, an acetylene flame was diluted with argon to reduce the carbonaceous matter emitted at the top of the

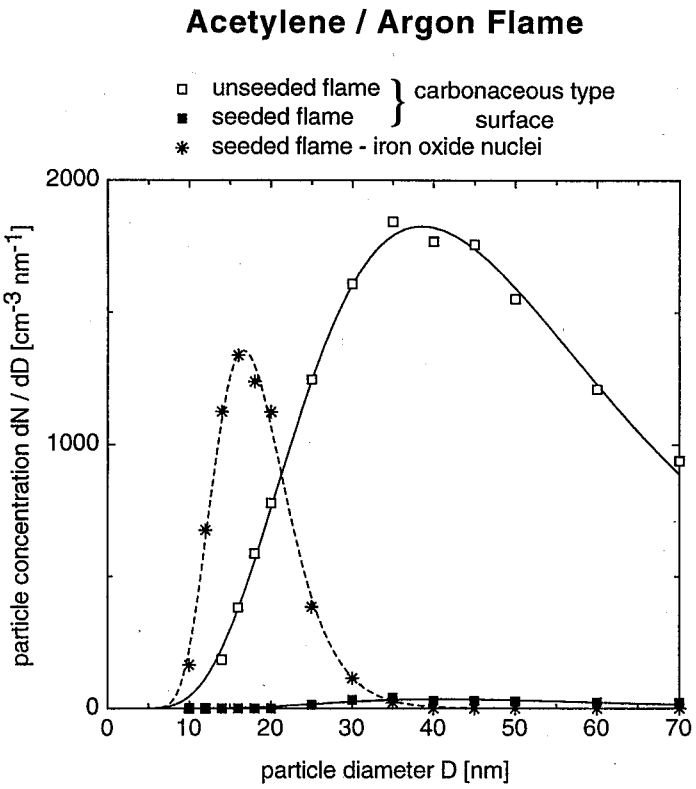

Figure 4: Particle size distributions above an acetylene/argon flame seeded and unseeded with ferrocene vapor. The carbonaceous particles are almost completely eliminated above the seeded flame.

flame to an acceptable level at which no clogging of the extraction pinhole occurred. Fig. 4 shows the size distribution of the carbonaceous particles above the visible height of the flame. When this flame is seeded with ferrocene vapor, the particles with a carbonaceous type surface disappear almost completely, while particles with iron oxide type surface reappear. The iron oxide nuclei size distribution is very similar to the one observed in the methane flame. Hence we see that the iron oxide nuclei formed from the ferrocene vapor act as condensation nuclei for carbonaceous matter, and at the end of the flame catalyze the burnout of the carbonaceous matter. This latter process is reminiscent of the production of iron from iron oxide and coal. Because metallic iron is pyrophoric in the form of small particles, the nuclei reoxidize once the catalytic burnout of the carbonaceous matter is completed.

Comparison to Diesel engines

The immissions of heavy duty construction engines have been tested as well with and without adding ferrocene to the fuel [1, 2].

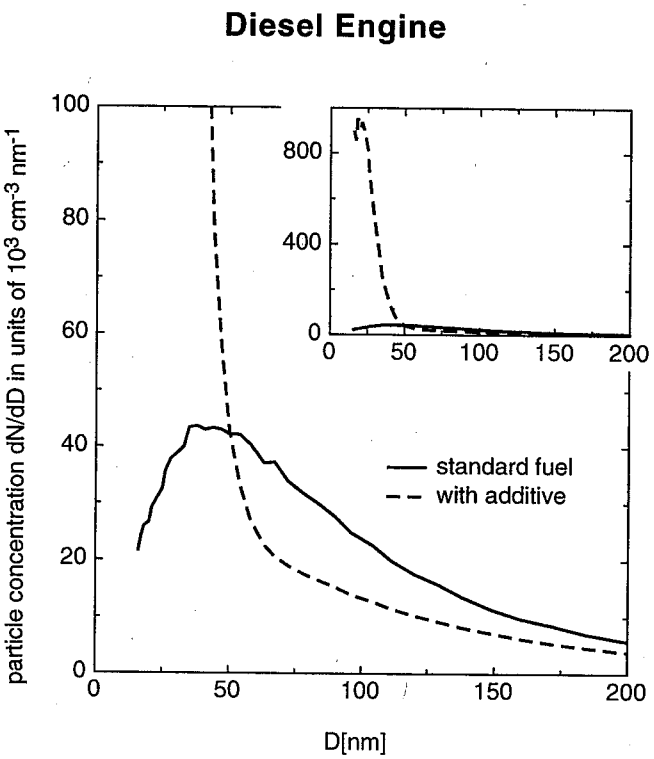

Figure 5: Particle size distributions in the diluted exhaust of a heavy duty diesel engine at full load. The small particles appearing when the diesel fuel is seeded with ferrocene have an extremely low photoelectric yield similar to the model experiment, but the burnout of the soot is far from complete, from [1, 2].

Fig. 5 shows the particle size distribution obtained after dilution. The fuel was commercially available diesel fuel seeded with the recommended amount of ferrocene (120 mg $Fe(C_5H_5)_2$/ kg standard diesel). The seeding induces a reduction of the carbonaceous particles of about 50%, but new particles with a smaller size appear in the exhaust. The new particles again have a very low photoelectric yield, and chemical analysis showed that they consist of iron oxides. Hence we observe just like in the model experiment that the additive ferrocene leads to the emission of finely dispersed iron oxide nuclei. The fact that the photoelectric yield is low shows that there is no carbonaceous matter left at the surface of these particles. Hence the catalytic burnout is just as effective as in the model combustion. Why is then so much carbonaceous matter left? It is likely that this arises because the iron oxide nuclei are not yet fully developed at the moment when carbonaceous matter is formed. Now iron oxide nuclei and carbonaceous particles cannot interact since they are not in contact. The removal of carbonaceous matter might therefore be improved by providing transition metal oxides or salts earlier in the combustion.

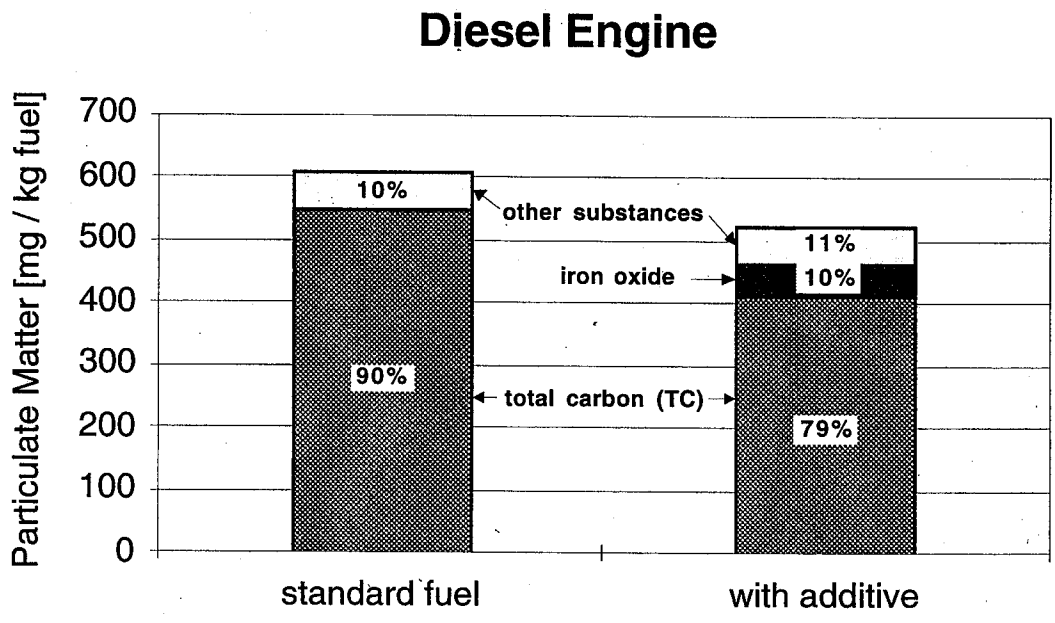

Figure 6: Comparison of total carbon (TC) and total particulate matter (PM) with and without fuel additive emitted by the engine of Fig. 5. While PM is hardly affected, TC is significantly reduced; from [1, 2].

Fig. 6 shows the more traditional results of immission analysis. Total carbon (TC), and total particulate matter (PM) have been measured under the same conditions as in Fig. 5 and also with and without adding the recommended amount of ferrocene to "standard diesel fuel". It appears that the seeding with ferrocene reduces PM only slightly, whereas the amount of TC shows an over-proportional decrease. This arises because the iron oxide nuclei from the seeding are added to the particulate immissions. In fact, the iron oxide mass calculated from the initial iron mass in the seeded fuel exactly matches the observed 10% "mass gap". As a result, the mass of these nuclei happens to almost compensate the reduction of carbonaceous matter that is generated by the fuel additive. On the other hand, we see that the additive was effective since it reduced TC as expected. In conclusion we state that the phenomena observed in the model experiment are also present in the more complicated and less transparent case of the real diesel engine. We also see that all the carbonaceous matter that condensed on the nuclei provided by the additive is burnt as desired. Yet a relatively large amount of carbonaceous matter is left unburnt. In the absence of more elegant solution, it then makes sense to precipitate all remaining particles in a filter where the soot comes in physical contact with the transition metal oxide and the catalytic burnout can be completed.

Acknowledgements - We wish to thank A. Mayer, J. Czerwinski and U. Matter for giving us the data about the diesel engine.

References

[1] Matter, U., Czerwinski, J., Mosimann, T., and Mayer, A. (1997). Penetration of Diesel Particle Filters evaluated by various Soot Analyzing Techniques. *Proceedings of the Workshop "Particle Measurement" at ETH Zuerich*, August 7, 1997.

[2] Matter, U. and Siegmann, K. (1997). The Influence of Particle Filter and Fuel Additives on Turbo Diesel Engine Exhaust. *J. Aerosol Sci.*, in print.

[3] Siegmann, K., Hepp, H. and Sattler, K. (1995). Reactive Dimerization: A New PAH Growth Mechanism in Flames. *Combust. Sci. and Tech.*, **109**, 165-181.

[4] Kasper, M., Siegmann, K. and Sattler, K. (1997). Evaluation of an in-situ Sampling Probe for its Accuracy in Determining Particle Size Distributions from Flames. *J. Aerosol Sci.*, in print.

[5] Hepp, H. and Siegmann, K. (1997). Mapping of Soot Particles in a Weakly Sooting Diffusion Flame by Aerosol Techniques. *Combustion and Flame*, accepted for publication.